Renewable Energy 186 (2022) 341–349

Contents lists available at ScienceDirect

Renewable Energy

journal homepage: www.elsevier.com/locate/renene

Double integrating *XYL2* into engineered *Saccharomyces cerevisiae* strains for consistently enhanced bioethanol production by effective xylose and hexose co-consumption of steam-exploded lignocellulose in bioenergy crops

Boyang He [a, b], Bo Hao [a, c], Haizhong Yu [b], Fen Tu [a, c], Xiaoyang Wei [a, b], Ke Xiong [a, c], Yajun Zeng [a, b], Hu Zeng [a, b], Peng Liu [a, b], Yuanyuan Tu [a, b], Yanting Wang [a, b], Heng Kang [a, b], Liangcai Peng [a, b], Tao Xia [a, c, *]

[a] *Biomass & Bioenergy Research Centre, College of Plant Science & Technology, Huazhong Agricultural University, Wuhan, 430070, China*
[b] *Laboratory of Biomass Engineering & Nanomaterial Application in Automobiles, College of Food Science & Chemical Engineering, Hubei University of Arts & Science, Xiangyang, China*
[c] *College of Life Science & Technology, Huazhong Agricultural University, Wuhan, 430070, China*

ARTICLE INFO

Article history:
Received 22 February 2021
Received in revised form
16 November 2021
Accepted 19 December 2021
Available online 27 December 2021

Keywords:
Saccharomyces cerevisiae
Gene integration
Xylose fermentation
Bioethanol production
Steam explosion
Bioenergy crops

ABSTRACT

Cellulosic ethanol has been regarded as excellent additive into petrol fuels for reduced net carbon release, and yeast fermentation is thus a crucial step for bioethanol production. In this study, three (*XYL1*/*Candida tropicalis*, *XYL2*/*Candida tropicalis*, *XKS1*/*Saccharomyces cerevisiae*) genes were isolated to construct four novel vectors using gene fusion and tandem technology. Four constructs were then transformed into common *Saccharomyces cerevisiae* strain, leading to varied and limited xylose utilization. While two representative constructs were transformed into industrial yeast strain (SF7), the engineered SF7-Ft3 strain could consume 95% of total xylose for ethanol yield at 2.08 g/L, whereas the control strain only utilized 13% xylose with ethanol yield at 0.56 g/L. Additional *XYL2* overexpression into the SF7-Ft3 strain led to consistently enhanced xylose utilization by from diverse enzymatic hydrolats of steam-exploded lignocellulose residues in three major bioenergy crops (wheat, maize, *Miscanthus*). These consequently increased bioethanol yields (% dry matter) and concentrations (g/L) by 11%–42%. Therefore, this study has demonstrated an applicable yeast-engineering approach for efficient xylose consumption and also provided a powerful strategy for enhancing bioethanol production in bioenergy crops.

1. Introduction

A great attention has been paid to the use of lignocellulose biomass for the production of biofuels and chemicals, because it is of enormous resource and non-conflict with food security [1,2]. In particular, bioethanol has been considered as the promising second generation of bioenergy for the partial replacement of fossil fuels [3]. In principle, lignocellulose process involves in three major stages: biomass pretreatment for wall polymer destruction, sequential enzymatic saccharification for soluble sugars release and final yeast fermentation for ethanol production [4–6]. As lignocellulose is of recalcitrant property against enzymatic hydrolysis, cost-effective and green-like biomass pretreatment is considered for enhancing sequential enzymatic hydrolysis to release hexoses and xylose as carbon source for yeast fermentation [7]. However, because classic yeast strain could not consume xylose for ethanol fermentation, it becomes essential to select genetic engineered yeast strains for xylose utilization [8,9].

Lignocellulose recalcitrance is in principle determined by plant cell wall composition (cellulose, hemicellulose, lignin, pectin), wall polymer feature and wall interlink network style [10,11]. To reduce the recalcitrance, physical and chemical pretreatments have been implemented with various biomass residues [12]. Particularly,

* Corresponding author. Biomass & Bioenergy Research Centre, College of Plant Science & Technology, Huazhong Agricultural University, Wuhan, 430070, China., .
E-mail address: xiatao@mail.hzau.edu.cn (T. Xia).
URL: http://bbrc.hzau.edu.cn

https://doi.org/10.1016/j.renene.2021.12.103
0960-1481/

steam explosion is increasingly applied as a relatively cost-effective and environment-friendly pretreatment by partially extracting hemicellulose and reducing cellulose degree of polymerization [13,14]. Meanwhile, as hemicellulose consists of more than 90% xylose, attempts have been made to engineer the yeast strains enabled for co-fermentation of hexoses and xylose [15–17].

Saccharomyces cerevisiae is one of the most effective ethanol-producing organisms by using hexoses as carbon source [18]. In terms of the xylose utilization, genetic engineering has been recently conducted to select the transgenic *S. cerevisiae* strains including the introduction of xylose metabolism and xylose transport [19,20], change of intracellular redox balance and over-expression of the genes involved in the pentose phosphate pathways [21,22]. Characteristically, xylose reductase (XR), xylitol dehydrogenase (XDH) and xylulose kinase (XK) are major enzymes for the pentose pyrophosphate pathways, whereas XYL1 and XYL2 respectively encode XR and XDH [23,24]. Hence, xylose is converted into xylulose via a two-step enzymatic reaction catalyzed by XR and XDH, and xylulose is then phosphorylated by XK as xylulose-5-phosphate via the pentose phosphate pathway and glycolysis [25,26]. However, pentose fermentation suffers from crucial limitations, due to the low expression of these genes and the imbalance in the redox cofactors [27,28].

Despite that the *S. cerevisiae* strain could be engineered by expressing XYL1 and XYL2, it exhibits a slow xylose fermentation and low ethanol yield, due to xylitol excretion [29]. Xylitol excretion is distinctive in the coenzyme specificities between XR and XDH and creates an intracellular redox imbalance [30]. XR has a higher affinity for NADPH than for NADH, and XDH exclusively uses NAD^+, resulting in the excess in NADH accumulation and a shortage of NAD^+ in the XDH reaction [31]. Attempts have been made to reduce the unwanted xylitol excretion by optimizing the XDH/XR activity ratio in the recombinant strains [32,33]. Modification of the gene-expression vectors is also attempted to enhance XR activity by changing the linker and/or the order between XYL1 and XYL2 genes. For instance, it has been reported that specific activities of two enzymes are dependent on the fusion protein order and the connecting region composition [34]. In addition, the linker length of several engineered chimerical proteins is critical for biological activity, dependent on correct folding in polyfunctional AROM enzyme [35]. However, much remains unknown about if the linking style of major enzymes could significantly improve xylose utilization for ethanol fermentation in engineered yeast strains.

In the present study, we designed diverse constructs for optimal expressions of XYL1, XYL2 and XKS1 in common *S. cerevisiae* and industrial engineered strains by using gene fusion and tandem technology, and then compared xylose-fermentation rates and bioethanol yields. Notably, this study performed steam explosion pretreatments with three major bioenergy crops (wheat, maize, *Miscanthus*) and determined much raised bioethanol production by combining additional XYL2-overexpressed engineered yeast strain with different solid/liquid ratio of enzymatic hydrate substrates, providing an integrated strategy for yeast engineering and lignocellulose processing for bioethanol production.

2. Materials and methods

2.1. Yeast strains and culture media

Candida tropicalis was used for *XYL1* and *XYL2* gene cloning as described in Supplementary Table S1, whereas the *S. cerevisiae* PY001 (MM476, MAT*a, pep4–3, leu2, trp1, ura3–52, prb1–1122*) was a parent strain for genetic engineering. The SF7 strain (*S. cerevisiae*) was collected from a factory, which is of adaptation to high temperature (37–42 °C) incubation and to high dosages of sugar (500 g/L glucose), salt (50 g/L NaCl) and ethanol (20 g/L) as well. All yeast strains were cultured in the YP medium (10 g/L yeast extract, 20 g/L peptone) with different concentrations of glucose and xylose.

2.2. Plasmids construction

XYL1 and *XYL2* were isolated from *Candida tropicalis* (ACCC: 20005) and *XKS1* was cloned from *S.cerevisiae* (MM476). The plasmids for intracellular constitution were constructed by using pYPGE15 with *PGK* promoters and *CYC1* terminator as described in Supplementary Table S2. Diverse fusion proteins (e.g, glycine-glycine-glycine-glycine-serine as G_4S_1) were designed, and all plasmids were constructed by PCR reactions including pYPGE15 (*PGKp-XYL1-CYC1t*), pYPGE15 (*PGKp-XYL2-CYC1t*), pYPGE15 (*PGKp-XKS1-CYC1t*), pYPGE15 (*PGKp-XYL1-CYC1t, PGKp-XYL2-CYC1t, PGKp-XKS1-CYC1t*), pYPGE15 (*PGKp-XYL2-CYC1t, PGKp-XYL1-CYC1t, PGKp-XKS1-CYC1t*), pYPGE15 (*PGKp-XYL1*$(G_4S_1)_1$*XYL2-CYC1t, PGKp-XKS1-CYC1t*) and pYPGE15 (*PGKp-XYL1*$(G_4S_1)_3$*XYL2- CYC1t, PGKp-XKS1-CYC1t*). The plasmids pAUR101 (*PGKp-XYL1*$(G_4S_1)_3$*XYL2-CYC1t, PGKp-XKS1-CYC1t*) and pAUR101 (*PGKp-XYL2-CYC1t, PGKp-XYL1-CYC1t, PGKp-XKS1-CYC1t*) were constructed from pYPGE15 (*PGKp-XYL1*$(G_4S_1)_3$*XYL2- CYC1t, PGKp-XKS1-CYC1t*) and pYPGE15 (*PGKp-XYL2-CYC1t, PGKp-XYL1-CYC1t, PGKp-XKS1-CYC1t*). The plasmids pPIC (*PGKp-XYL2-CYC1t*) was constructed from pYPGE15 (*PGKp-XYL2-CYC1t*).

2.3. Yeast transformation

The lithium acetate method was applied for yeast transformation with the plasmids constructed above [36], and all obtained strains were described in Supplementary Table S3.

2.4. Enzyme activity assay

Cell extracts were prepared for activity assays of the three xylose metabolic enzymes. One colony was inoculated into 3 mL SC medium at 30 °C on a rotary shaker at 200 rpm for 12 h, and 5 μL of the culture was transferred to a 250 mL flask containing 50 mL SC. After incubated at 30 °C with shaking at 200 rpm for 24–36 h, all cells were harvested by centrifugation at 4000*g* for 5 min at 4 °C, washed with sterile, deionized H_2O three times and re-suspended in 5 mL sterile normal saline for 30 min ice bath. The cells were inoculated into a set of a 250 mL flask containing 50 mL SC to reach an OD600 with 0.1 and incubated at 30 °C with shaking at 200 rpm for 96 h. Cells were harvested every 12 h by centrifugation at 4000*g* for 5 min at 4 °C. After washed with deionized H_2O three times, the cells were re-suspended in 0.1 M sodium phosphate buffer with an equal volume of glass beads, the diameter of which is 0.5 mm. The cells were shaken under vortex for 1 min after 1 min ice-bath, and repeated for 15 times. Then, the lysate was centrifuged at 12000 *g* for 10 min at 4 °C, and the supernatant was collected for enzyme assays in new tube supplemented with equal volume of ice-bath glycerol.

All enzyme activities were measured using fresh extracts. XYL1 activity measurement was performed spectrophotometrically by determining the oxidation of NADPH under 340 nm at 30 °C. The reaction mixture included 100 mM sodium phosphate buffer (pH 7.0), 2 mM xylose and 1.2 mM NADPH [37]. XYL2 activity was accounted by measuring the oxidation of NAD^+ under 340 nm at 30 °C in the reaction mixture (100 mM Tris-HCl pH 7.0, 1.0 mM $MgCl_2$, 5.0 mM NAD^+, 50 mM xylitol). XKS1 activity was assayed by monitoring the oxidation of NADH under 340 nm at 30 °C in the reaction mixture (50 mM Tris-HCl pH 7.5, 2.0 mM $MgCl_2$, 0.2 mM NADH, 8.5 mM xylulose, 0.2 mM phosphoenol pyruvate, 10 U pyruvate kinase, 10 U lactate dehydrogenase, 2.0 mM adenosine

triphosphate) [38]. All assays were conducted in independent triplicate.

2.5. Yeast fermentation

Ethanol fermentations were carried out under an anaerobic condition as previously described [39]. The pre-cultured yeast cells (aerobically grown in 100 mL of YPD medium containing 20 g/L of glucose for 2 days at 30 °C with orbital shaking at 150 rpm) were harvested by centrifugation at 1000*g* for 5 min. The yeast cells were re-suspended in the fermentation media to initiate fermentation with a starting OD600 of 0.5. The oxygen-limited fermentation was performed at 30 °C under shaken at 70 rpm for 96 h for PY001 and engineered strains. The oxygen-limited fermentation was performed at 37 °C under shaken at 150 rpm for 48 h or longer for SF7 and engineered industrial strains. During the fermentation, the supernatant was filtered by one-off filter (0.22 μm) for analysis of substrates and products.

2.6. Steam explosion pretreatment of three bioenergy crop straws

The dried crop straws were cut into the 5–8 cm size, sprayed with deionized water to the moisture at 50% (w/v) and pretreated under steam explosion by loading 400 g wet biomass materials into 5 L steam explosion reactor (QBS-200, Hebi Zhengdao Machine Factory, Hebi, China). The steam explosion conditions were established for wheat (2.5 Pa, 180 s), maize (2.0 Pa, 180 s) and *Miscanthus* (2.5 Pa, 180 s), and the steam exploded (SE) residues were then used for enzymatic hydrolysis and fermentation as previously described [40].

2.7. Enzymatic hydrolysis and bioethanol measurement

The SE biomass samples were incubated with mixed-cellulases (0.04 g/g DW, Imperial Jade Biotechnology Co., Ltd. Ningxia, China) containing Tween-80 at 0.4 mL/g dry matter. The sealed samples were shaken under 150 rpm for 48 h at 50 °C at different solid–liquid ratios. After centrifugation at 3000*g* for 5 min, the supernatants were collected for yeast fermentation. The fermentation liquid was distilled at 100 °C, and appropriate amount of purify ethanol sample in 2 mL 5% $K_2Cr_2O_7$ was heated for 10 min in a boiling water bath, and the ethanol was accounted as previously described [40].

2.8. Wall polymer assay

Plant cell wall fractionation was performed to extract soluble sugars, pectin, hemicellulose and cellulose fractions as previously described [40,41]. A UV-VIS spectrometer (V-1100D, Shanghai MAPADA Instruments Co.) was used for hexoses and pentoses assays as previously described [42]. For cellulose assay, the sample was dissolved in 67% H_2SO_4 and hexoses were calculated by the anthrone/H_2SO_4 method. Hemicelluloses were calculated by determining total hexoses and pentoses of the hemicellulose fraction. The two-step acid hydrolysis method was applied for total lignin assay according to the Laboratory Analytical Procedure of the National Renewable Energy Laboratory as described [43]. All experiments were completed in independent triplicate.

2.9. Monosaccharide determination

Monosaccharide determination was conducted by GC/MS (SHIMADZU GCMS-QP2010 Plus) using Restek Rxi-5ms, 30 m × 0.25 mm ID × 0.25 μm df column as previously described [44]. The mass spectrometer was operated in the EI mode with ionization energy of 70 eV. Calibration curves of all analytes routinely yielded correlation coefficients at 0.999 or better.

2.10. Real-time PCR analysis

The transcription levels of *XYL1*, *XYL2* and *XKS1* were accounted by real-time PCR assay as described [45]. Total RNA was extracted by Trizol reagent (Tiangen Biotech, Beijing, China) and reverse transcribed to cDNA using EasyScript One-Step gDNA Removal and cDNA Synthesis SuperMiX (TransGen Biotech, Beijing, China). qRT-PCR was conducted using a BioRad IQ5 real-time PCR system. The PCR thermal cycle conditions included one cycle of 95 °C for 2 min, followed by 45 cycles of 95 °C for 15 s, 55 °C for 15 s, and 72 °C for 25 s. Gene *ACT1* for actin was used as an internal control. The primers for the RT-PCR are described in Supplementary Table S4. All assays were performed in independent triplicate.

3. Results and discussion

3.1. Diverse integrations of XYL1, XYL2 and XKS1 genes for high enzyme activities in yeast strain

In this study, we initially isolated *XYL1* (975 bp) and *XYL2* (1,095 bp) from *Candida tropicalis* and *XKS1* (1,803 bp) from *S. cerevisiae* MM476 (Supplementary Table 1). To express *XYL1*, *XYL2*, and *XKS1* genes in *S. cerevisiae* MM476, diverse plasmids were generated from seven intermediate constructs (Fig. 1A). In the pYPGE15*XYL1XYL2XKS1* (Tf3) and pYPGE15*XYL2XYL1XKS1* (Tr3) plasmids, *XYL1* and *XYL2* genes were positioned in a reverse order, whereas *XKS1* was placed behind the *XYL1* and *XYL2* fragments. In the pYPGE15*XYL1*–$(G_4S_1)_1$–*XYL2XKS1* (Fs3) and pYPGE15*XYL1*–$(G_4S_1)_3$–*XYL2XKS1* (Ft3) plasmids, *XYL1* and *XYL2* were constructed to encode the fusion proteins with different length linkers. In particular, plasmid pYPGE15*XYL1*–$(G_4S_1)_1$–*XYL2XKS1* encoded an in-frame fusion of *XYL1* and *XYL2* with five amino acids (G_4S_1) in the connecting region, while plasmid pYPGE15*XYL1*–$(G_4S_1)_3$–*XYL2XKS1* contained a longer linker of fifteen amino acids $(G_4S_1)_3$.

The constructed plasmids were transformed into *S. cerevisiae* MM476, and the empty vector (pYPGE15) was used as control (Table S1). The transformants were selected and assayed for protein expression by SDS-PAGE (Fig. 1B). Each encoded protein (XR, XDH, and XK) had a strong band that corresponded to the predicted molecular weight in the strains that expressed the individual XYL1, XYL2, and XKS1, compared with that of the empty vector strain (EV). In the strain that co-expressed all three genes (XYL1-XYL2XKS1), more XR than XDH and XK proteins was detected. By comparison, the XYL2XYL1XKS1 strain showed a relatively higher proportion of XDH and lower XR than the XYL1XYL2XKS1 strain. Similar results were also found between the XYL1XYL2 and XYL2XYL1 strains (data not shown). Hence, the yeast strain positioning of XYL1 or XYL2 at the front yielded relatively higher protein products.

With respect to the yeast strains that express the XYL1–XYL2 fusion genes, we detected their predicted protein bands. The XYL1–$(G_4S_1)_1$–XYL2XKS1 strain produced much higher fusion protein level than the XYL1–$(G_4S_1)_3$–XYL2XKS1 strain did, and a similar result was found between the XYL1–$(G_4S_1)_1$–XYL2 and XYL1–$(G_4S_1)_3$–XYL2 strains (data not shown). This result indicated that the increase in the linker length (amino acid numbers) between the two genes could reduce the fusion protein expression level.

Extracts of the *S. cerevisiae* strains were used for the XR, XDH, and XK enzyme activity assay *in vitro*. To measure three XR, XDH and XK enzyme activities, we selected four yeast strains either by co-expressing XYL1, XYL2, and XKS1 or by expressing the

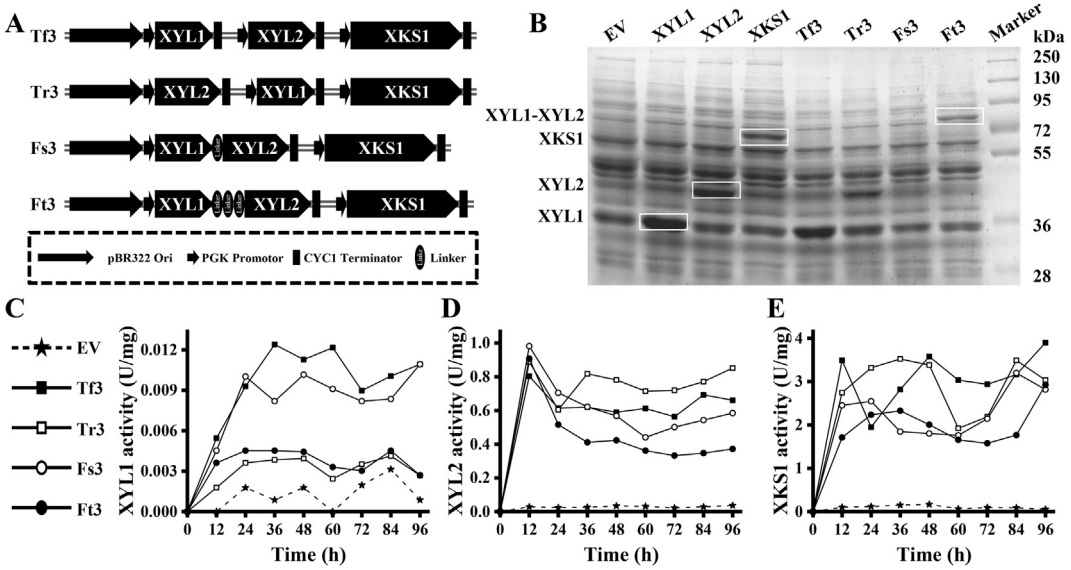

Fig. 1. Integration of *XYL1*, *XYL2* and *XKS1* with common *S. cerevisiae* strain (PY001). (A) Schematic diagrams of four vectors for distinct three (*XYL1*, *XYL2* and *XKS1*) genes construction. (B) SDS-PAGE profiling of XYL1, XYL2 and XKS1 proteins in engineered yeast strains. (C, D, E) Enzyme activity assay *in vitro* of XYL1, XYL2 and XKS1 in four engineered yeast strains and control (empty vector/EV).

XYL1−XYL2 fusion genes with XKS1 as described above (Fig. 1C−E). During the incubation, the XYL1XYL2XKS1 strain (Tf3) had a much higher XR activity than the XYL2XYL1XKS1 strain (Tr3) did (Fig. 1C). Similarly, the XYL1−$(G_4S_1)_1$−XYL2XKS1 strain (Fs3) also showed a higher XR activity than the XYL1−$(G_4S_1)_3$−XYL2XKS1 strain (Ft3). In comparison, the XDH activities were much higher in the four strains than the XR activities (Fig. 1B). Furthermore, either Tr3 or Fs3 strain retained a relatively higher XDH activity than the other two strains (Tf3, Ft3; Fig. 1E), which confirmed that positioning the gene front or reducing the fusion gene linker length could increase the protein levels and enzyme activities. However, the XDH/XR activity ratio values in both theTr3 and Ft3 strains were much higher than those of the Fs3 and Tf3 strains. In addition, all the four strains had a higher XDH/XR activity ratio, compared with the control strain (EV); the Tf3 and Fs3 strains displayed an almost similar ratio during the incubation time. Hence, the data suggested an approach for balancing the XR and XDH enzyme activities to reduce the xylitol formation during the xylose fermentation in yeast. With regard to the XK enzyme activity, all four yeast strains showed much higher activities than those of the control strain (Fig. 1E). However, during the incubation, the maximum XK activities in the Tf3 and Tr3 strains were higher than those of the Fs3 and Ft3 strains. Hence, the selected four yeast strains were of largely varied enzymes (XR, XDH, XK) activities.

3.2. Varied xylose co-fermentation rates for bioethanol production in engineered yeast strains

To compare the xylose co-fermentation rates among the yeast strains generated above, this study performed yeast fermentation in the medium that contains 60 g/L xylose and 25 g/L glucose under oxygen-limited condition at 30 °C (Fig. 2). During the fermentation, the glucose could be completely used after 36 h in all four engineered yeast strains and the control (EV), whereas the xylose was initially consumed in three strains (Tr3, Fs3, Ft3), other than in Tf3 and EV strains (Figs. 2A−B). After 96 h fermentation, those three strains consistently consumed more xylose than that of the EV, but the Tf3 did not show much different xylose consumption capacity. Furthermore, this study determined that all four engineered strains could produce higher bioethanol yields (g/L) than that of the EV, in particular on the Tf3 and Ft3 strains after 96 h fermentation (Fig. 2C). Hence, despite that the xylose consumption was limited in the engineered strains, the results suggested that integration of *XYL1*, *XYL2* and *XKS1* genes could lead to enhanced ethanol fermentation in the yeast strains examined.

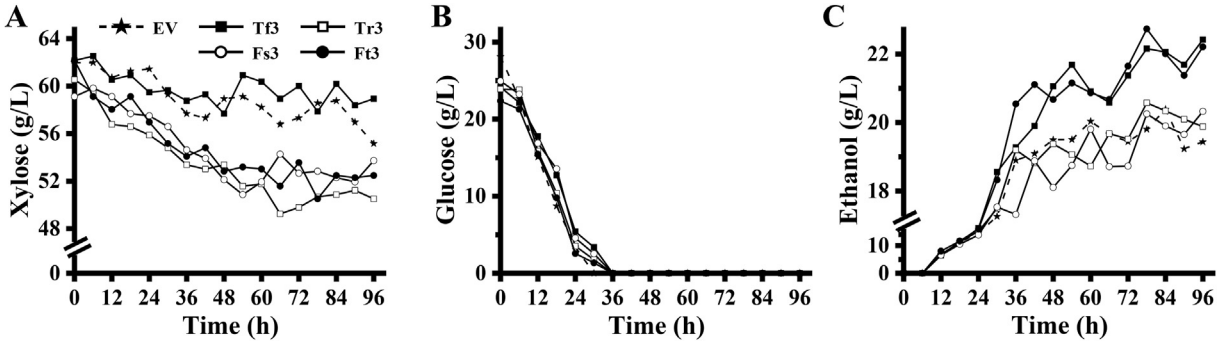

Fig. 2. Time course analyses of xylose and hexose consumption for bioethanol production in four engineered yeast strains and control (EV). (A) Xylose unconsumed by yeast strains. (B) Glucose consumed by yeast strains. (C) Bioethanol released by yeast strains by co-consumption of 25 g/L glucose and 60 g/L xylose at 30 °C under oxygen-limited fermentation.

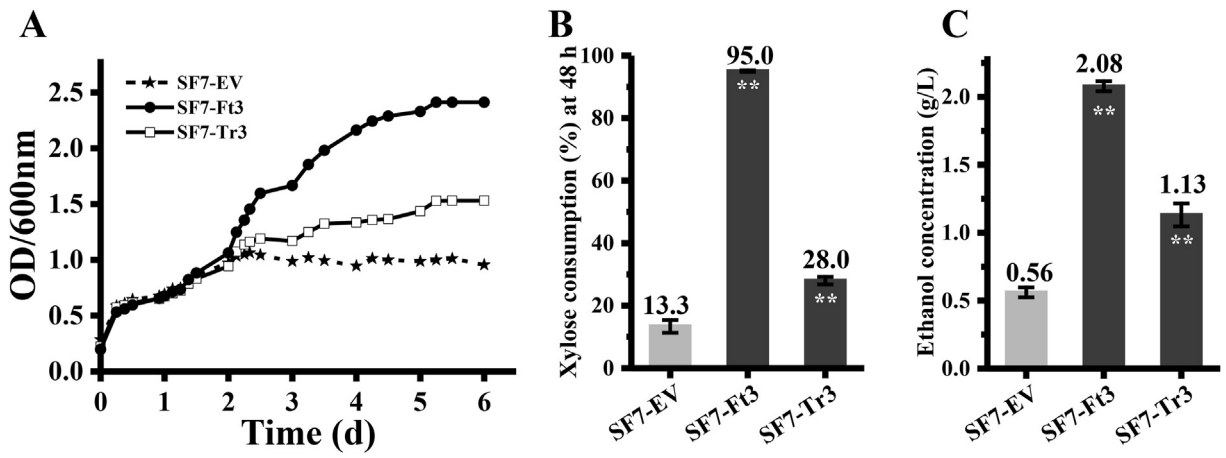

Fig. 3. Characterization of xylose consumption for bioethanol production in engineered industrial *S. cerevisiae* strains (SF7-Ft3; SF7-Tr3). (A) Time course observation of yeast cell growth with the culture media containing 20 g/L xylose only in two engineered industrial strains and EV. (B, C) Xylose consumption rate (of total) and bioethanol concentration (g/L) by two engineered industrial strains and EV with the synthetic medium containing 45 g/L xylose as sole carbon source after 48 h fermentation. **As significant difference by *t*-test between engineered strains and EV at $p < 0.01$ level (n = 3).

3.3. Enhanced xylose consumption for bioethanol production in engineered industry yeast strains

To further examine the integration of *XYL1*, *XYL2* and *XKS1* genes for xylose consumption and bioethanol production, this study transformed two representative constructs (Ft3, Tr3) into the industry yeast stain (SF7) that is of high ethanol fermentation capacity [46]. While incubated with the culture media containing 20 g/L xylose as a sole carbon source, two engineered industrial trains (SF7-Ft3, SF7-Tr3) exhibited a much faster growth with significantly higher OD/600 nm values than those of the control/empty vector (SF7-EV; Fig. 3A). Particularly, the SF7-Ft3 stain could even show much higher OD value than that of the SF7-Tr3. Meanwhile, this study detected that the SF7-Tr3 and SF7-Ft3 strains were of much raised xylose consumption rates, which were 2- and 7 folds higher than those of the SF7-EV, respectively (Fig. 3B). Notably, the SF7-Ft3 showed a xylose consumption of 95%. As a consequence, the SF7-Tr3 and SF7-Ft3 strains could respectively produce bioethanol yields of 1.13 g/L and 2.08 g/L, whereas the SF7-EV strain had the ethanol yield of 0.56 g/L (Fig. 3C). The results hence indicated that the integration of *XYL1*, *XYL2* and *XKS1* genes could lead to much enhanced xylose consumption for higher bioethanol production in the engineered industrial strains, even though hexose is absent during ethanol fermentation. It has also suggested that the overproduction of XYL2 in the SF7-Ft3 and SF7-Tr3 strains should be a major factor on xylose consumption capacity for bioethanol productivity, which is consistent with the previous assumption [47].

3.4. Additional XYL2 overexpression for further increased xylose utilization of the enzymatic hydrates of steam-exploded residues in three major bioenergy crops

As XYL2 could play a major role in xylose consumption for bioethanol production [34], this study further generated the SF7-Ft3-X2 strain that additionally over-expressed XYL2 gene in the SF7-Ft3 strain (Fig. 4). Compared to the SF7-Tr3 and SF7-Ft3 strains, the SF7-Ft3-X2 strain was of much higher *XYL2* transcription level up to 3–4 folds (Fig. 4A), leading to a consistently enhanced yeast cell growth while incubated with xylose as carbon source only (Fig. 4B).

To examine specific xylose utilization capacity of the engineered yeast strains, this study applied the soluble sugars released from enzymatic hydrolyses of the steam-exploded lignocellulose residues of three major bioenergy crops (wheat, maize, *Miscanthus*) consisting of reduced hemicellulose and relatively increased cellulose and lignin (Table 1). Using total soluble sugars containing diverse xylose (covering 94%–97% of total) levels (Supplementary Table S5) from the enzymatic hydrolyses of lignocellulose substrates at different solid-liquid ratios (1:5; 1:10; 1:20), we examined that the SF7-Ft3-X2 strain had much more pentose utilization than those of the control, being up to 4-fold in the solid-liquid (1:5) substrate of *Miscanthus* (Table 2). Notably, the SF7-Ft3-X2 strain remained significantly more pentose utilization than the SF7-Ft3 strains at the most hydrates examined, indicating that additional overexpression of *XYL2* could enhance yeast cell growth and xylose consumption capacity.

3.5. Consistently enhanced bioethanol yields and concentrations by integrative-engineered yeast strain for diverse hydrate substrates of three bioenergy crops

Because the SF7-Ft3-X2 strain is of high xylose consumption capacity for the enzymatic hydrates of steam-exploded lignocellulose residues in three major bioenergy crops as described above, this study determined their bioethanol production such as bioethanol yield (% dry matter) and concentration (g/L; Fig. 5). Although bioethanol production was largely varied among different solid/liquid rates of enzymatic hydrates, the SF7-Ft3-X2 strain produced much higher bioethanol yields or concentrations than those of the control (SF7-EV) in all samples examined, with raised bioethanol yields and concentrations by 11%–42% (Fig. 5A-F). Further compared to the SF7-Ft3 strain, the SF7-Ft3-X2 strain remained significantly increased bioethanol production in total eight samples, except for the wheat hydrate sample of solid/liquid at 1:20.

With respect to the SF7-Ft3-X2 strain that is of high bioethanol productivity, we examined hexoses consumption rates of all nine enzymatic hydrates samples in three bioenergy crops (Table 3). As a comparison, a similar hexoses utilization rate was found among three yeast strains in all wheat steam-exploded substrates, whereas the SF7-Ft3-X2 strain showed slightly higher hexoses consumption than those of the SF7-Ft3 and SF7-EV strains in all maize and two *Miscanthus* samples, being different from the above findings that the SF7-Ft3-X2 was of consistently higher xylose consumption in

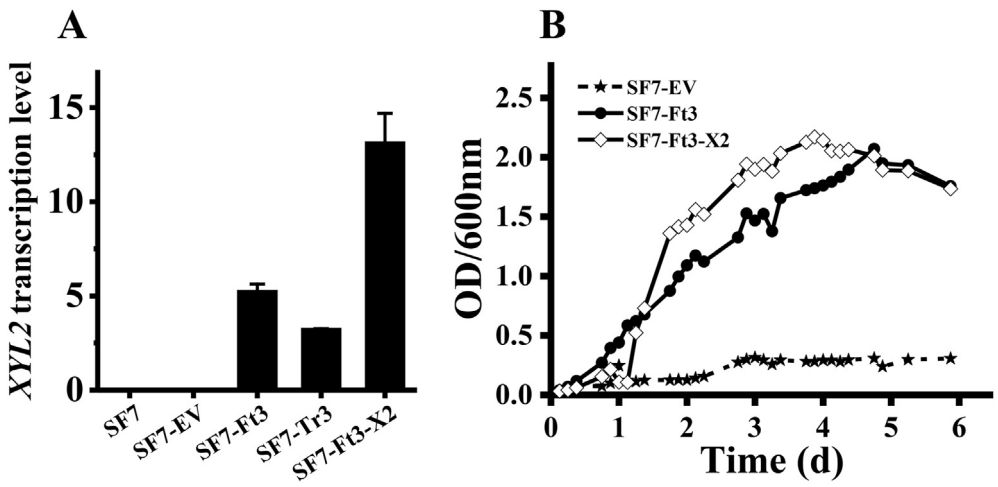

Fig. 4. Identification of additional overexpression of *XYL2* gene in engineered industrial SF7-Ft3-X2 strain. (A) *XYL2* transcription levels in three engineered industrial strains and controls (SF7-EV, SF7); gene *ACT1* used as an internal control; bars indicated as the relative gene expression levels. (B) Time course observation of yeast cell growth of two engineered industrial strains and control with the culture media containing 20 g/L xylose and 20 g/L glucose as carbon sources.

Table 1
Cell wall composition (% dry matter) of steam-exploded residues in bioenergy crops.

Samples	Cell wall composition (% dry matter)		
	Cellulose	Hemicellulose	Lignin
Wheat	33.66 ± 0.99[a]	10.74 ± 0.38	40.16 ± 0.71
Maize	44.69 ± 1.00	13.78 ± 0.05	35.30 ± 0.72
Miscanthus	41.90 ± 0.94	11.12 ± 0.34	30.53 ± 0.75

[a] Data as mean ± SD (n = 3).

all nine hydrates samples examined (Table 2). Hence, the results suggested that the increased bioethanol productivity should be mainly due to more xylose consumption by the SF7-Ft3-X2 strain in total eight enzymatic hydrates samples of three bioenergy crops examined. Exceptionally, the SF7-Ft3-X2 strain exhibited much higher consumption capacities of both xylose and hexoses than those of the SF7-EV strain in the *Miscanthus* hydrate sample of solid/liquid at 1:5 (Table 3), leading to the most raised bioethanol yield and concentration among total nine hydrate samples of three bioenergy crops (Fig. 5C & F). However, it remains to test what is the optimal hydrate for a complete xylose and hexose consumption by the SF7-Ft3-X2 strain in the future studies. On the other hand, the bioethanol yields and concentrations achieved by the SF7-Ft3-X2 strain were relatively lower than those of the previously-reported [48], which should be mainly due to an incomplete enzymatic hydrolysis and relatively high lignin composition of the steam-exploded residues in three bioenergy crops. Hence, it will be interesting to explore the optimal biomass process technology for maximum bioethanol production by the SF7-Ft3-X2 strain in bioenergy crops.

Table 2
Pentose consumption (% dry weight) by engineered yeast strains for yeast fermentation under different solid-liquid ratios of steamed-explored lignocellulose residues of three bioenergy crops.

Yeast strain	Solid-liquid ratio		Solid-liquid ratio		Solid-liquid ratio	
	1:5		1:10		1:20	
	Pentose concentration (% dry matter)	Pentose utilization (% of total)	Pentose concentration (% dry matter)	Pentose utilization (% of total)	Pentose concentration (% dry matter)	Pentose utilization (% of total)
Wheat						
Non-fermentation	11.48 ± 0.07[a]		12.13 ± 0.11		12.14 ± 0.06	
SF7-EV	9.07 ± 0.16	20.92 ± 1.16[a]	8.85 ± 0.13	27.04 ± 0.86[a]	8.81 ± 0.23	27.50 ± 1.55[a]
SF7-Ft3	7.47 ± 0.09	34.87 ± 0.63[b]	8.28 ± 0.20	31.72 ± 1.37[b]	8.02 ± 0.22	33.96 ± 1.51[b]
SF7-Ft3-X2	7.28 ± 0.21	36.57 ± 1.47[b]	8.06 ± 0.11	33.51 ± 0.72[b]	7.77 ± 0.30	36.00 ± 1.98[b]
Maize						
Non-fermentation	8.82 ± 0.09		9.31 ± 0.06		9.59 ± 0.07	
SF7-EV	6.17 ± 0.33	29.96 ± 3.06[a]	5.94 ± 0.10	36.15 ± 0.85[a]	6.45 ± 0.23	32.66 ± 2.00[a]
SF7-Ft3	5.93 ± 0.14	32.78 ± 1.31[a]	5.76 ± 0.06	38.07 ± 0.54[a]	5.64 ± 0.24	41.18 ± 2.09[b]
SF7-Ft3-X2	5.16 ± 0.06	41.51 ± 0.57[b]	5.29 ± 0.15	43.16 ± 1.33[b]	5.23 ± 0.13	45.39 ± 1.09[b]
Miscanthus						
Non-fermentation	6.56 ± 0.19		7.41 ± 0.17		8.96 ± 0.11	
SF7-EV	5.95 ± 0.17	9.23 ± 2.10[a]	5.59 ± 0.06	24.65 ± 0.71[a]	6.15 ± 0.13	31.35 ± 1.21[a]
SF7-Ft3	5.13 ± 0.19	21.79 ± 2.40[b]	5.41 ± 0.11	27.06 ± 1.26[a]	5.72 ± 0.06	36.16 ± 0.59[b]
SF7-Ft3-X2	4.13 ± 0.26	37.02 ± 3.21[c]	4.73 ± 0.18	36.23 ± 1.99[b]	4.65 ± 0.19	48.09 ± 1.70[c]

[a] Data as mean ± SD (n = 3).

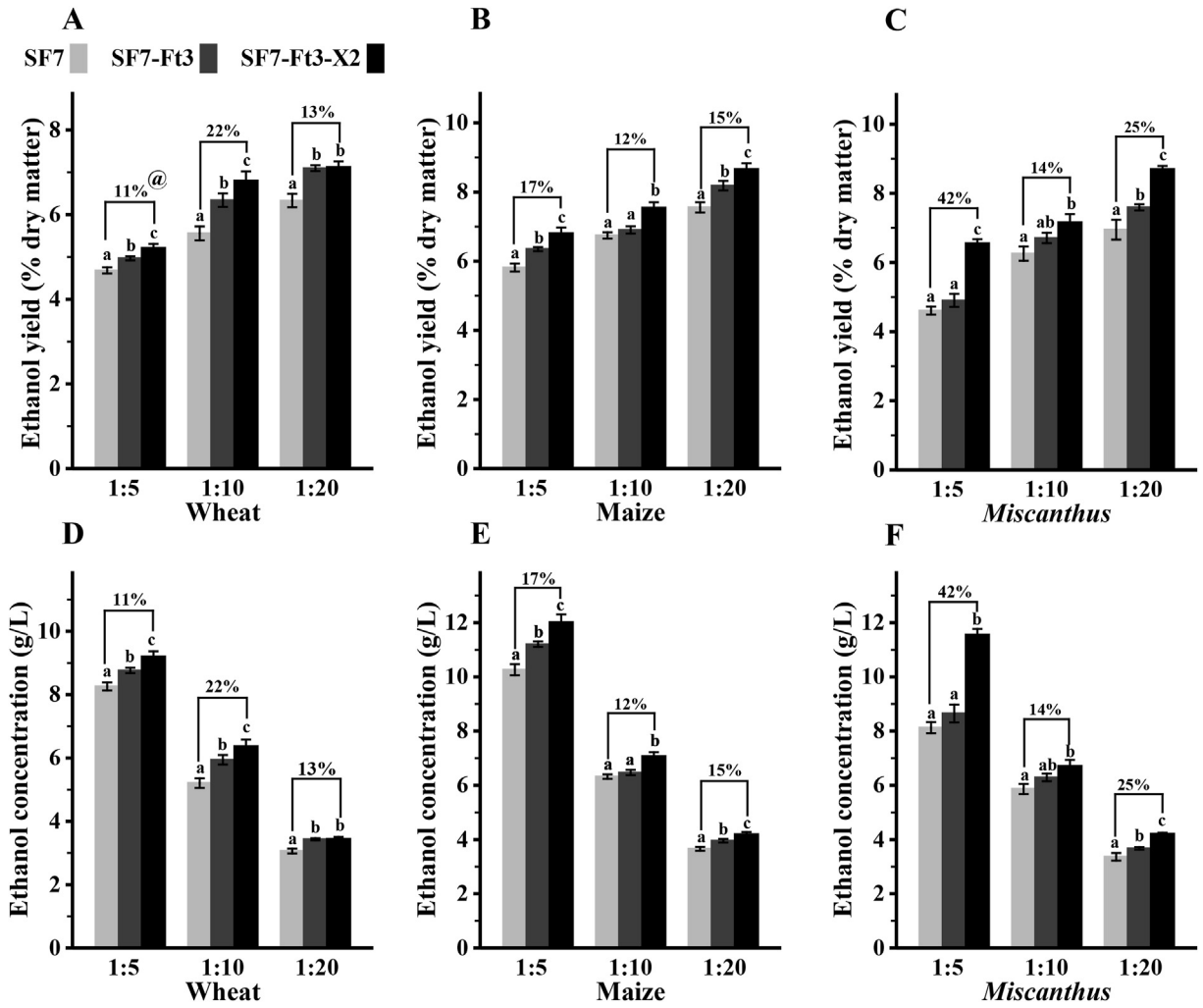

Fig. 5. Comparison of bioethanol production between two engineered industrial yeast strains and control using total soluble sugars released by enzymatic hydrolyses of steam-exploded lignocellulose residues of different solid-liquid ratios (1:5; 1:10, 1:20) in three bioenergy crops (wheat, maize and *Miscanthus*). (A, B, C) Bioethanol yields (% dry matter) by yeast fermentation for 48 h. (D, E, F) Bioethanol concentrations (g/L) by yeast fermentation for 48 h. Letter ^{a,b,c} as multiple *t*-test at $p < 0.05$ level (n = 3) among two engineered yeast strains and control (EV) strain; @As raised bioethanol yield or concentration by engineered strain against the control (EV) strain.

4. Conclusions

By designing fusion and tandem technology, this study generated four novel constructs to express three genes (*XYL1*, *XYL2*, *XKS1*) in common *Saccharomyces cerevisiae* and industrial engineered strain (SF7), which are effective for xylose consumption and bioethanol conversion. The engineered SF7-Ft3 strain could consume 95% xylose for significantly raised ethanol yield up to 3.7 folds, compared to its control stain. Notably, the optimal SF7-Ft3-X2 strain could balance XDH/XR activity ratio to further enhance xylose utilization from the enzymatic hydrates of steam-exploded lignocellulose residues in three major bioenergy crops (wheat, maize, *Miscanthus*), which respectively led to the bioethanol yield and concentration increased up to 22%, 17% and 42%. Hence, this study has provided a useful strategy for bioethanol production by combining engineered yeast strain with green-like biomass processing in bioenergy crops.

CRediT authorship contribution statement

Boyang He: Investigation, Methodology, Formal analysis, Software, Writing – original draft. **Bo Hao:** Conceptualization, Methodology. **Haizhong Yu:** Writing - review & editing, Formal analysis. **Fen Tu:** Investigation, Writing - review & editing. **Xiaoyang Wei:** Investigation, Formal analysis. **Ke Xiong:** Investigation, Methodology. **Yajun Zeng:** Validation, Software. **Hu Zeng:** Investigation, Data curation. **Peng Liu:** Validation, Writing - review & editing. **Yuanyuan Tu:** Formal analysis, Validation, Writing - review & editing. **Yanting Wang:** Validation, Project administration. **Heng Kang:** Conceptualization, Methodology. **Liangcai Peng:** Conceptualization, Writing - review & editing, Supervision. **Tao Xia:** Conceptualization, Writing – original draft, Writing - review & editing, Funding acquisition, All authors agreed to state that the data of manuscript were true from independent experiments performed in this study.

Declaration of competing interest

The authors declare that they have no known competing financial interests or personal relationships that could have appeared to influence the work reported in this paper.

Table 3
Hexose consumption (% dry weight) by engineered yeast strains for yeast fermentation under different solid-liquid ratios of steamed-explored lignocellulose residues of three bioenergy crops.

Yeast strain	Solid-liquid ratio		Solid-liquid ratio		Solid-liquid ratio	
	1:5		1:10		1:20	
	Hexose concentration (% dry matter)	Hexose utilization (% of total)	Hexose concentration (% dry matter)	Hexose utilization (% of total)	Hexose concentration (% dry matter)	Hexose utilization (% of total)
Wheat						
Non-fermentation	14.38 ± 0.20[a]		16.21 ± 0.27		17.76 ± 0.14	
SF7-EV	2.28 ± 0.10	84.18 ± 0.55[a]	2.61 ± 0.10	83.88 ± 0.51[a]	2.58 ± 0.11	85.50 ± 0.49[a]
SF7-Ft3	2.36 ± 0.10	83.60 ± 0.56[a]	2.66 ± 0.08	83.59 ± 0.39[a]	2.63 ± 0.05	85.21 ± 0.21[a]
SF7-Ft3-X2	2.20 ± 0.06	84.72 ± 0.35[a]	2.63 ± 0.06	83.75 ± 0.30[a]	2.52 ± 0.10	85.83 ± 0.46[a]
Maize						
Non-fermentation	16.86 ± 0.03		18.78 ± 0.09		19.17 ± 0.18	
SF7-EV	3.67 ± 0.27	78.20 ± 1.31[a]	2.69 ± 0.09	85.68 ± 0.39[a]	2.51 ± 0.13	86.90 ± 0.54[ab]
SF7-Ft3	3.46 ± 0.16	79.43 ± 0.77[a]	2.65 ± 0.04	85.88 ± 0.18[a]	2.66 ± 0.10	86.10 ± 0.43[a]
SF7-Ft3-X2	2.95 ± 0.06	82.50 ± 0.28[b]	2.40 ± 0.06	87.21 ± 0.28[b]	2.33 ± 0.08	87.84 ± 0.32[b]
Miscanthus						
Non-fermentation	14.13 ± 0.31		18.26 ± 0.07		23.26 ± 0.47	
SF7-EV	8.30 ± 0.11	41.26 ± 0.62[a]	4.24 ± 0.13	76.81 ± 0.60[a]	4.40 ± 0.15	81.09 ± 0.54[a]
SF7-Ft3	7.07 ± 0.17	49.99 ± 1.01[b]	4.18 ± 0.22	77.14 ± 0.98[a]	3.77 ± 0.11	83.81 ± 0.39[b]
SF7-Ft3-X2	3.83 ± 0.24	72.89 ± 1.41[c]	3.69 ± 0.18	79.79 ± 0.82[b]	3.76 ± 0.13	83.85 ± 0.45[b]

Letter [a,b,c] as multiple *t*-test at $p < 0.05$ level (n = 3) among two engineered yeast strains and control (EV) strain.
[a] Data as mean ± SD (n = 3).

Acknowledgments

This work was in part supported by the project of Huazhong Agricultural University Independent Scientific & Technological Innovation Foundation (2662020ZKPY013; 2662019PY054), the National 111 Project of Ministry of Education of China (BP0820035) and the Project of Hubei University of Arts & Science (XKQ2018006).

Appendix A. Supplementary data

Supplementary data to this article can be found online at https://doi.org/10.1016/j.renene.2021.12.103.

References

[1] X. Wang, Q.N. He, Y.F. Yang, J.W. Wang, K. Haning, Y. Hu, B. Wu, M.X. He, Y.P. Zhang, J. Bao, L.M. Contreras, S.H. Yang, Advances and prospects in metabolic engineering of *Zymomonas mobilis*, Metab. Eng. 50 (2018) 57–73, https://doi.org/10.1016/j.ymben.2018.04.001.
[2] W.C. Li, J.Q. Zhu, X. Zhao, L. Qin, T. Xu, X. Zhou, X. Li, B.Z. Li, Y.J. Yuan, Improving co-fermentation of glucose and xylose by adaptive evolution of engineering xylose-fermenting *Saccharomyces cerevisiae* and different fermentation strategies, Renew. Energy 139 (2019) 1176–1183, https://doi.org/10.1016/j.renene.2019.03.028.
[3] J.A. Bañuelos, I. Velázquez-Hernández, M. Guerra-Balcázar, N. Arjona, Production, characterization and evaluation of the energetic capability of bioethanol from *Salicornia Bigelovii* as a renewable energy source, Renew. Energy 123 (2018) 125–134, https://doi.org/10.1016/j.renene.2018.02.031.
[4] Y.T. Wang, C.F. Fan, H.Z. Hu, Y. Li, D. Sun, Y.M. Wang, L.C. Peng, Genetic modification of plant cell walls to enhance biomass yield and biofuel production in bioenergy crops, Biotechnol. Adv. 34 (2016) 997–1017, https://doi.org/10.1016/j.biotechadv.2016.06.001.
[5] M. Madadi, Y.M. Wang, C.B. Xu, P. Liu, Y.T. Wang, T. Xia, Y.Y. Tu, X.C. Lin, B. Song, X.E. Yang, W.B. Zhu, D. Duanmu, S.W. Tang, L.C. Peng, Using *Amaranthus* green proteins as universal biosurfactant and biosorbent for effective enzymatic degradation of diverse lignocellulose residues and efficient multiple trace metals remediation of farming lands, J. Hazard Mater. 406 (2020), 124727, https://doi.org/10.1016/j.jhazmat.2020.124727.
[6] A. van Eerde, A. Várnai, J.K. Jameson, L. Paruch, A. Moen, J.H. Anonsen, P. Chylenski, H.S. Steen, I. Heldal, R. Bock, V.G.H. Eijsink, J.H. Liu-Clarke, In-depth characterization of *Trichoderma reesei* cellobiohydrolase *TrCel7A* produced in *Nicotiana benthamiana* reveals limitations of cellulase production in plants by host-specific post-translational modifications, Plant Biotechnol. J. 18 (2020) 631–643, https://doi.org/10.1111/pbi.13227.
[7] Y.M. Wang, P. Liu, G.F. Zhang, Q.M. Yang, J. Lu, T. Xia, L.C. Peng, Y.T. Wang, Cascading of engineered bioenergy plants and fungi sustainable for low-cost bioethanol and high-value biomaterials under green-like biomass processing, Renew. Sustain. Energy Rev. 137 (2021), 110586, https://doi.org/10.1016/j.rser.2020.110586.
[8] D.N. Moysés, V.C. Reis, J.R. de Almeida, L.M. de Moraes, F.A. Torres, Xylose fermentation by *Saccharomyces cerevisiae*: challenges and prospects, Int. J. Mol. Sci. 17 (2016) 207–224, https://doi.org/10.3390/ijms17030207.
[9] G. Trausinger, C. Gruber, S. Krahulec, C. Magnes, B. Nidetzky, M. Klimacek, Identification of novel metabolic interactions controlling carbon flux from xylose to ethanol in natural and recombinant yeasts, Biotechnol. Biofuels 8 (2015) 157–169, https://doi.org/10.1186/s13068-015-0340-x.
[10] L.M. Wu, S.Q. Feng, J. Deng, B. Yu, Y.M. Wang, B.Y. He, H. Peng, Q. Li, R.F. Hu, L.C. Peng, Altered carbon assimilation and cellulose accessibility to maximize bioethanol yield under low-cost biomass processing in corn brittle stalk, Green Chem. 21 (2019) 4388–4399, https://doi.org/10.1039/c9gc01237k.
[11] C. Bonatto, B. Venturin, D.A. Mayer, S.F. Bazoti, D. de Oliveira, S.L. Alves, H. Treichel, Experimental data and modelling of 2G ethanol production by *Wickerhamomyces* sp. UFFS-CE-3.1.2, Renew. Energy 145 (2020) 2445–2450, https://doi.org/10.1016/j.renene.2019.08.010.
[12] J. Deng, X.B. Zhu, P. Chen, B.Y. He, S.W. Tang, W.Y. Zhao, X.L. Li, R. Zhang, Z.Y. Lv, H. Kang, L. Yu, L.C. Peng, Mechanism of lignocellulose modification and enzyme disadsorption for complete biomass saccharification to maximize bioethanol yield in rapeseed stalks, Sustain. Energy Fuels 4 (2020), https://doi.org/10.1039/c9se00906j.
[13] J.D. DeMartini, M. Foston, X. Meng, S. Jung, R. Kumar, A.J. Ragauskas, C.E. Wyman, How chip size impacts steam pretreatment effectiveness for biological conversion of poplar wood into fermentable sugars, Biotechnol. Biofuels 8 (2015) 209–224, https://doi.org/10.1186/s13068-015-0373-1.
[14] D. Sun, A. Alam, Y.Y. Tu, S.G. Zhou, Y.T. Wang, T. Xia, J.F. Huang, Y. Li, Zahoor, X.Y. Wei, B. Hao, L.C. Peng, Steam-exploded biomass saccharification is predominately affected by lignocellulose porosity and largely enhanced by Tween-80 in *Miscanthus*, Bioresour. Technol. 239 (2017) 74–81, https://doi.org/10.1016/j.biortech.2017.04.114.
[15] K.J. Dussán, D.D.V. Silva, V.H. Perez, S.S. da Silva, Evaluation of oxygen availability on ethanol production from sugarcane bagasse hydrolysate in a batch bioreactor using two strains of xylose-fermenting yeast, Renew. Energy 87 (2016) 703–710, https://doi.org/10.1016/j.renene.2015.10.065.
[16] P.J. Slininger, R.J. Bothast, J.E. van Cauwenberge, C.P. Kurtzman, Conversion of D-xylose to ethanol by the yeast *Pachysolen tannophilus*, Biotechnol. Bioeng. 24 (1982) 371–384, https://doi.org/10.1002/bit.260240210.
[17] P.J. Slininger, R.J. Bothast, M.R. Okos, M.R. Ladisch, Comparative evaluation of ethanol production by xylose-fermenting yeasts presented high xylose concentrations, Biotechnol. Lett. 7 (1985) 431–436, https://doi.org/10.1007/BF01166218.
[18] T. Yu, Y.J. Zhou, M.T. Huang, Q.L. Liu, R. Pereira, F. David, J. Nielsen,

Reprogramming yeast metabolism from alcoholic fermentation to lipogenesis, Cell 174 (2018) 1549–1558, https://doi.org/10.1016/j.cell.2018.07.013.
[19] C.E. Costa, A. Romaní, J.T. Cunha, B. Johansson, L. Domingues, Integrated approach for selecting efficient *Saccharomyces cerevisiae* for industrial lignocellulosic fermentations: importance of yeast chassis linked to process conditions, Bioresour. Technol. 227 (2017) 24–34, https://doi.org/10.1016/j.biortech.2016.12.016.
[20] A.A. Kamoldeen, C.K. Lee, W.N. Wan Abdullah, C.P. Leh, Enhanced ethanol production from mild alkali-treated oil-palm empty fruit bunches via co-fermentation of glucose and xylose, Renew. Energy 107 (2017) 113–123, https://doi.org/10.1016/j.renene.2017.01.039.
[21] G. Scalcinati, J.M. Otero, J.R. van Vleet, T.W. Jeffries, L. Olsson, J. Nielsen, Evolutionary engineering of *Saccharomyces cerevisiae* for efficient aerobic xylose consumption, FEMS Yeast Res. 12 (2012) 582–597, https://doi.org/10.1111/j.1567-1364.2012.00808.x.
[22] P.H. Tran, J.K. Ko, G. Gong, Y. Um, S.M. Lee, Improved simultaneous co-fermentation of glucose and xylose by *Saccharomyces cerevisiae* for efficient lignocellulosic biorefinery, Biotechnol. Biofuels 13 (2020) 12–25, https://doi.org/10.1186/s13068-019-1641-2.
[23] E.J. Oh, S.J. Ha, S. Rin Kim, W.H. Lee, J.M. Galazka, J.H. Cate, Y.S. Jin, Enhanced xylitol production through simultaneous co-utilization of cellobiose and xylose by engineered *Saccharomyces cerevisiae*, Metab. Eng. 15 (2013) 226–234, https://doi.org/10.1016/j.ymben.2012.09.003.
[24] J.H. Jo, Y.C. Park, Y.S. Jin, J.H. Seo, Construction of efficient xylose-fermenting *Saccharomyces cerevisiae* through a synthetic isozyme system of xylose reductase from *Scheffersomyces stipitis*, Bioresour. Technol. 241 (2017) 88–94, https://doi.org/10.1016/j.biortech.2017.05.091.
[25] A. Madhavan, A. Srivastava, A. Kondo, V.S. Bisaria, Bioconversion of lignocellulose-derived sugars to ethanol by engineered *Saccharomyces cerevisiae*, Crit. Rev. Biotechnol. 32 (2012) 22–48, https://doi.org/10.3109/07388551.2010.539551.
[26] Y. Kobayashi, T. Sahara, S. Ohgiya, Y. Kamagata, K.E. Fujimori, Systematic optimization of gene expression of pentose phosphate pathway enhances ethanol production from a glucose/xylose mixed medium in a recombinant *Saccharomyces cerevisiae*, AMB Express 8 (2018) 139–149, https://doi.org/10.1186/s13568-018-0670-8.
[27] A. Cadière, A. Ortiz-Julien, C. Camarasa, S. Dequin, Evolutionary engineered *Saccharomyces cerevisiae* wine yeast strains with increased in vivo flux through the pentose phosphate pathway, Metab. Eng. 13 (2011) 263–271, https://doi.org/10.1016/j.ymben.2011.01.008.
[28] H.C. Veras, C.G. Campos, I.F. Nascimento, P.V. Abdelnur, J.R. Almeida, N.S. Parachin, Metabolic flux analysis for metabolome data validation of naturally xylose-fermenting yeasts, BMC Biotechnol. 19 (2019) 58, https://doi.org/10.1186/s12896-019-0548-0.
[29] J. Zha, M.H. Shen, M.L. Hu, H. Song, Y.J. Yuan, Enhanced expression of genes involved in initial xylose metabolism and the oxidative pentose phosphate pathway in the improved xylose-utilizing *Saccharomyces cerevisiae* through evolutionary engineering, J. Ind. Microbiol. Biotechnol. 41 (2014) 27–39, https://doi.org/10.1007/s10295-013-1350-y.
[30] S. Kwak, J.H. Jo, E. Yun, Y.S. Jin, J.H. Seo, Production of biofuels and chemicals from xylose using native and engineered yeast strains, Biotechnol. Adv. 37 (2019) 271–283, https://doi.org/10.1016/j.biotechadv.2018.12.003.
[31] N.S. Parachin, B. Bergdahl, E.W. van Niel, M.F. Gorwa-Grauslund, Kinetic modelling reveals current limitations in the production of ethanol from xylose by recombinant *Saccharomyces cerevisiae*, Metab. Eng. 13 (2011) 508–517, https://doi.org/10.1016/j.ymben.2011.05.005.
[32] S.R. Kim, Y.C. Park, Y.S. Jin, J.H. Seo, Strain engineering of *Saccharomyces cerevisiae* for enhanced xylose metabolism, Biotechnol. Adv. 31 (2013) 851–861, https://doi.org/10.1016/j.biotechadv.2013.03.004.
[33] M. Klimacek, S. Krahulec, U. Sauer, B. Nidetzky, Limitations in xylose-fermenting *Saccharomyces cerevisiae*, made evident through comprehensive metabolite profiling and thermodynamic analysis, Appl. Environ. Microbiol. 76 (2010) 7566–7574, https://doi.org/10.1128/AEM.01787-10.
[34] M. Anderlund, P. Rådström, B. Hahn-Hägerdal, Expression of bifunctional enzymes with xylose reductase and xylitol dehydrogenase activity in *Saccharomyces cerevisiae* alters product formation during xylose fermentation, Metab. Eng. 3 (2001) 226–235, https://doi.org/10.1006/mben.2001.0190.
[35] I.J. Purvis, A.J.E. Bettany, T.C. Santiago, J.R. Coggins, K. Duncan, R. Eason, A.J.P. Brown, The efficiency of folding of some proteins is increased by controlled rates of translation *in vivo*: a hypothesis, J. Mol. Biol. 193 (1987) 413–417, https://doi.org/10.1016/0022-2836(87)90230-0.
[36] D. Gietz, A.S. Jean, R.A. Woods, R.H. Schiestl, Improved method for high efficiency transformation of intact yeast cells, Nucleic Acids Res. 20 (1992) 1425, https://doi.org/10.1093/nar/20.6.1425.
[37] K.L. Smiley, P.L. Bolen, Demonstration of D-xylose reductase and D-xylitol dehydrogenase in *Pachysolen tannophilus*, Biotechnol. Lett. 4 (1982) 607–610, https://doi.org/10.1007/BF00127793.
[38] A. Eliasson, C. Christensson, C.F. Wahlbom, B. Hahn-Hägerdal, Anaerobic xylose fermentation by recombinant *Saccharomyces cerevisiae* carrying *XYL1*, *XYL2*, and *XKS1* in mineral medium chemostat cultures, Appl. Environ. Microbiol. 66 (2000) 3381–3386, https://doi.org/10.1128/aem.66.8.3381-3386.2000.
[39] L.L. Cheng, L.Q. Wang, L.Y. Wei, Y. Wu, A. Alam, C.B. Xu, Y.T. Wang, Y.Y. Tu, L.C. Peng, T. Xia, Combined mild chemical pretreatments for complete cadmium release and cellulosic ethanol co-production distinctive in wheat mutant straw, Green Chem. 21 (2019) 3693–3700, https://doi.org/10.1039/c9gc00686a.
[40] W.X. Jin, L. Chen, M. Hu, D. Sun, A. Li, Y. Li, Z. Hu, S.G. Zhou, Y.Y. Tu, T. Xia, Y.T. Wang, G.S. Xie, Y.B. Li, B.W. Bai, L.C. Peng, Tween-80 is effective for enhancing steam-exploded biomass enzymatic saccharification and ethanol production by specifically lessening cellulase absorption with lignin in common reed, Appl. Energy 175 (2016) 82–90, https://doi.org/10.1016/j.apenergy.2016.04.104.
[41] L.C. Peng, C.H. Hocart, J.W. Redmond, R.E. Williamson, Fractionation of carbohydrates in *Arabidopsis* root cell walls shows that three radial swelling loci are specifically involved in cellulose production, Planta 211 (2000) 406–414, https://doi.org/10.1007/s004250000301.
[42] J.F. Huang, T. Xia, A. Li, B. Yu, Q. Li, Y.Y. Tu, W. Zhang, Z.L. Yi, L.C. Peng, A rapid and consistent near infrared spectroscopic assay for biomass enzymatic digestibility upon various physical and chemical pretreatments in *Miscanthus*, Bioresour. Technol. 121 (2012) 274–281, https://doi.org/10.1016/j.biortech.2012.06.015.
[43] G.F. Zhang, L.Q. Wang, X.K. Li, S.M. Bai, Y.L. Xue, Z.H. Li, S.W. Tang, Y.T. Wang, Y.M. Wang, Z. Hu, P. Li, L.C. Peng, Distinctively altered lignin biosynthesis by site-modification of *OsCAD2* for enhanced biomass saccharification in rice, GCB Bioenergy 13 (2020) 305–319, https://doi.org/10.1111/gcbb.12772.
[44] Y.T. Wang, J.F. Huang, Y. Li, K. Xiong, Y.M. Wang, F.C. Li, M.Y. Liu, Z.L. Wu, Y.Y. Tu, L.C. Peng, Ammonium oxalate-extractable uronic acids positively affect biomass enzymatic digestibility by reducing lignocellulose crystallinity in *Miscanthus*, Bioresour. Technol. 196 (2015) 391–398, https://doi.org/10.1016/j.biortech.2015.07.099.
[45] R. Zhang, H.Z. Hu, Y.M. Wang, Z. Hu, S. Ren, J.Y. Li, B.Y. He, Y.T. Wang, T. Xia, P. Chen, G.S. Xie, L.C. Peng, A novel rice *fragile culm 24* mutant encodes a UDP-glucose epimerase that affects cell wall properties and photosynthesis, J. Exp. Bot. 71 (2020) 2956–2969, https://doi.org/10.1093/jxb/eraa044.
[46] Zahoor, Y.Y. Tu, L.Q. Wang, T. Xia, D. Sun, S.G. Zhou, Y.T. Wang, Y. Li, H.P. Zhang, T. Zhang, M. Madadi, L.C. Peng, Mild chemical pretreatments are sufficient for complete saccharification of steam-exploded residues and high ethanol production in desirable wheat accessions, Bioresour. Technol. 243 (2017) 319–326, https://doi.org/10.1016/j.biortech.2017.06.111.
[47] S.R. Kim, S.J. Ha, I.I. Kong, Y.S. Jin, High expression of *XYL2* coding for xylitol dehydrogenase is necessary for efficient xylose fermentation by engineered *Saccharomyces cerevisiae*, Metab. Eng. 14 (2012) 336–343, https://doi.org/10.1016/j.ymben.2012.04.001.
[48] L. Zhu, P.S. Li, T.M. Sun, M.L. Kong, X.W. Li, S. Ali, W.B. Liu, S.C. Fan, J.C. Qiao, S.Z. Li, L.C. Peng, B.Y. He, M.J. Jin, W. Xiao, L.M. Cao, Overexpression of *SFA1* in engineered *Saccharomyces cerevisiae* to increase xylose utilization and ethanol production from different lignocellulose hydrolysates, Bioresour. Technol. 313 (2020), 123724, https://doi.org/10.1016/j.biortech.2020.123724.